

Improving optical performance of inverted organic solar cells by microcavity effect

Yongbing Long

Citation: [Applied Physics Letters](#) **95**, 193301 (2009); doi: 10.1063/1.3262967

View online: <http://dx.doi.org/10.1063/1.3262967>

View Table of Contents: <http://scitation.aip.org/content/aip/journal/apl/95/19?ver=pdfcov>

Published by the [AIP Publishing](#)

Articles you may be interested in

[Toward high efficiency of inverted organic solar cells: Concurrent improvement in optical and electrical properties of electron transport layers](#)

Appl. Phys. Lett. **102**, 253111 (2013); 10.1063/1.4812981

[Improved cathode buffer layer to decrease exciton recombination in organic planar heterojunction solar cells](#)

Appl. Phys. Lett. **102**, 043301 (2013); 10.1063/1.4789852

[Highly flexible inverted organic solar cells with improved performance by using an ultrasmooth Ag cathode](#)

Appl. Phys. Lett. **101**, 133303 (2012); 10.1063/1.4755774

[Effect of the vertical composition gradient of active layer on the performance of bulk-heterojunction organic photovoltaic cell](#)

J. Appl. Phys. **110**, 114521 (2011); 10.1063/1.3666061

[Asymmetric tandem organic photovoltaic cells with hybrid planar-mixed molecular heterojunctions](#)

Appl. Phys. Lett. **85**, 5757 (2004); 10.1063/1.1829776

Confidently measure down to 0.01 fA and up to 10 PΩ

Keysight B2980A Series Picoammeters/Electrometers

[View video demo](#)



Improving optical performance of inverted organic solar cells by microcavity effect

Yongbing Long (龙拥兵)^{a)}

Department of Mathematics and Physics, Institute of Thin Film and Nanomaterial, WuYi University, Jiangmen 529020, People's Republic of China

(Received 6 September 2009; accepted 16 October 2009; published online 11 November 2009)

Optical simulations have been performed to investigate the performance of inverted organic solar cells with metal-mirror microcavity structure formed by central active layer sandwiched between semitransparent silver (Ag) cathode and thick Ag anode. Compared to nearly optimized noncavity devices with indium tin oxide cathode, the total absorbed photons (TAPs) in a 70 nm-thick active layer for cavity devices can be improved by 16.3% due to microcavity effect. Furthermore, an improvement of over 10% in TAPs can be obtained when thin Ag layer is optimized to be 10–16 nm thick, indicating thin Ag layer is a good choice as transparent electrode material. © 2009 American Institute of Physics. [doi:10.1063/1.3262967]

Organic solar cells (OSCs) based on bulk-heterojunction materials have received increasing attention within the last few years because of their advantages in low cost, flexibility, and light weight.^{1–3} In spite of these advantages, the OSC materials have an intrinsic drawback, poor electron-hole transport.⁴ This requires the active layer to be thin to shorten the distance for charge carrier transport and eventually reduce the probability of charge recombination. But, when the thickness of the active layer is reduced, the number of the photons absorbed by the active material decreases and less photocurrent is generated. Therefore, increasing the optical absorption in the thin active layer is an important issue in OSCs. Approaches developed for this purpose include microcavity,^{5,6} photonic crystals,⁷ plasmon couplers,⁸ and optical spacers.⁹ Another important issue for OSCs lies in the high cost of indium tin oxide (ITO) electrode material. To find alternatives for expensive ITO, investigation has been initiated on carbon nanotube conductive coatings,¹⁰ aluminum-doped zinc oxide,¹¹ metallic microgrids,¹² and thin metal transparent electrodes, in particular, have received increasing interest due to their low-cost roll-to-roll fabrication and excellent electrical performance.^{13–16}

This letter will address these issues by investigating the optical performance of inverted organic solar cell (IOSC) devices with metal-mirror microcavity structure formed by two silver (Ag) layers, where one is optically thick (anode) and the other is transparent (cathode). Optical simulations based on transfer matrix method (TMM)^{17–19} have been performed to compare the optical performance of the cavity devices with Ag transparent cathode and the noncavity devices with ITO cathode. The calculations indicate that optical performance of the adjusted cavity devices with thin active layer is enhanced significantly by the microcavity effect.

In the devices on which calculations have been performed, the active layer is assumed to be made from a blend of poly-3-hexylthiophene (P3HT) and [6,6]-phenyl-C61-butyric acid methyl ester (PCBM). ZnO and WO₃ layers are used as the electron transportance layer (ETL) and hole transportance layer, respectively. A thin tris(8-hydroxy-

quinolino)-aluminum (Alq₃) layer is capped on the thin silver cathode to increase the light coupling. All the optical constants of the materials involved in the calculations are extracted from Refs. 7 and 20–22.

Optical absorption in the cavity device is first calculated as a function of the wavelength and active layer thickness. And then the enhancement factor (EF) of the absorption is calculated as the ratio of the optical absorption in the cavity devices to the optical absorption in the noncavity devices with a structure of Glass/ITO(105 nm)/ZnO(10 nm)/P3HT:PCBM(0–300 nm) / WO₃(10 nm) / Ag(150 nm). The results of calculation are illuminated in Fig. 1. From the figure, two main results can be observed. First, light absorption for a given wavelength shows peaks with the increase in active layer thickness and high absorption (>90%) can be achieved over a wide spectrum (480–550 nm). In addition, compared to the noncavity devices with ITO cathodes, the optical absorption in the active layer for the cavity devices is improved at point A, C, and D, but reduced at point B.

To explain the results above, cavity resonance effect should be taken into consideration. A fraction of the incident light illuminated on the IOSC devices is reflected away from the device at one of the various entrance interfaces, and the

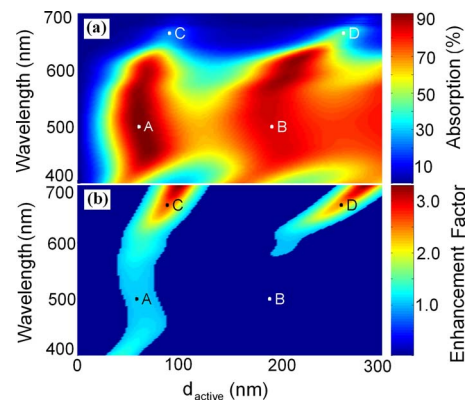


FIG. 1. (Color online) (a) Absorption vs wavelength and d_{active} for cavity device consisting of Alq₃(50 nm)/Ag(13 nm)/ZnO(10 nm)/P3HT:PCBM(0–300 nm)/WO₃(10 nm)/Ag(150 nm)/Glass; (b) EF of the optical absorption as a function of wavelength and d_{active} . The point where EF is less than one is not displayed.

^{a)} Author to whom correspondence should be addressed. Tel.: +86-750-329 9678. Electronic mail: yongbinglong@gmail.com.

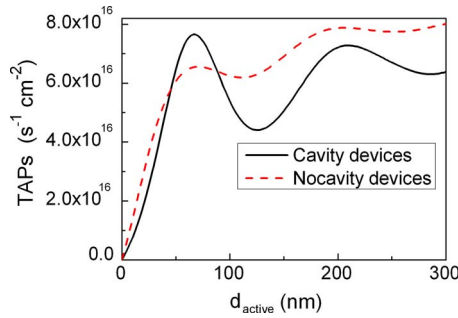


FIG. 2. (Color online) Number of TAPs in the active layer as a function of the active layer thickness. Black line: for cavity device consisting of $\text{Alq}_3(50 \text{ nm})/\text{Ag}(13 \text{ nm})/\text{ZnO}(10 \text{ nm})/\text{P3HT:PCBM}(0\text{--}300 \text{ nm})/\text{WO}_3(10 \text{ nm})/\text{Ag}(150 \text{ nm})/\text{Glass}$; and red dashed line: for non-cavity device consisting of $\text{Glass}/\text{ITO}(105 \text{ nm})/\text{ZnO}(10 \text{ nm})/\text{P3HT:PCBM}(0\text{--}300 \text{ nm})/\text{WO}_3(10 \text{ nm})/\text{Ag}(150 \text{ nm})$.

remaining light makes round trips between the two silver mirrors. When the light waves resulting from the multiple reflections at the silver mirrors interfere constructively, optical resonance will happen, leading to the maximum light absorption in the active layer.⁵ The optical resonant condition for the light with a given wavelength (λ) can be described as⁶

$$\sum_i n_i d_i + \frac{\lambda}{4\pi}(\psi_1 + \psi_2) = \frac{m\lambda}{2}, \quad (1)$$

where n_i and d_i are refractive index and thickness of the layers between two mirrors; ψ_1 and ψ_2 are the phase change upon reflection from the semitransparent Ag electrode and the thick Ag electrode; m is a positive integer. In Figs. 1(a) and 1(b), the region containing peak point A and C corresponds to the first-order resonance ($m=1$), and the region containing peak point B and D corresponds to the second-order resonance ($m=2$).

It has been pointed out that inserting a tailored mirror with high reflection between the glass and ITO layer can enhance the optical absorption where the active layer is a weak absorber but decrease the absorption where the active layer is a strong absorber.⁶ In the case of metal-mirror microcavity devices discussed in this letter, the thin Ag layer together with the Alq_3 layer act as a mirror with high reflection which can be tailored by changing the thicknesses of the Ag layer and Alq_3 layer. At point A, C, and D, the active layer is a weak absorber because the active layer is thin or the extinction coefficient is low. Therefore, the light absorption is improved when the Ag cathode with high reflectivity substitutes the ITO transparent cathode. But at point B, the absorption in the active layer is reduced because the active layer is a strong absorber.

The above analysis demonstrates that maximum value of the optical absorption in the active layer is dependent on both the wavelength and the active layer thickness. Therefore, to optimize the optical performance of the IOSC devices, a preferred way is to calculate the number of total absorbed photons (TAPs) in the active layer by integrating the absorbed photons for all wavelengths, and then maximize the integrated value by tailoring the thicknesses of active layer, HTL(WO_3), ETL(ZnO), as well as the thicknesses of the thin Ag layer and Alq_3 layer.

First, dependence of TAPs on the thickness of active layer is investigated and the results are displayed in Fig. 2. In

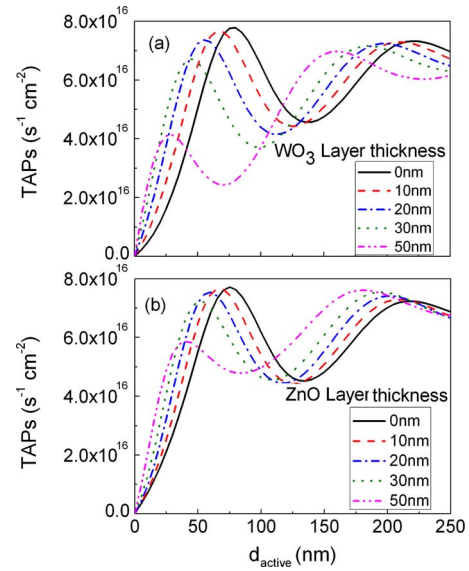


FIG. 3. (Color online) Number of TAPs in the active layer as a function of d_{active} . (a) For different thicknesses of WO_3 ; (b) for different thicknesses of ZnO .

the calculation, the number of TAPs is calculated by multiplying the spectrum response with the AM1.5 solar spectrum ($100 \text{ mW}/\text{cm}^2$). The figure demonstrates that the number of TAPs in the cavity device shows oscillated behavior with the peaks sharper than those in noncavity device (red dashed line). In addition, when compared to the noncavity devices, an enhancement in TAPs is achieved for cavity devices with the active layer thickness ranging from 50 to 85 nm, which corresponds to the first-order resonance. Furthermore, the largest enhancement (16.3%) occurs when the active layer is 70 nm thick, where the number of TAPs ($7.67 \times 10^{16} \text{ s}^{-1} \text{ cm}^{-2}$) is approaching that ($7.86 \times 10^{16} \text{ s}^{-1} \text{ cm}^{-2}$) in noncavity devices with 200 nm-thick active layer. The result is important for OSC design because reducing the thickness of the active layer from 200 to 70 nm can lower the probability of charge recombination and then improve the charge collection.

Second, investigation into the dependence of TAPs on the thicknesses of HTL(WO_3) and ETL (ZnO) has been performed and the results of calculations are depicted in Fig. 3. In the calculations, the layer thicknesses of Alq_3 and Ag transparent cathode are assumed to be 50 and 13 nm, respectively. Figures 3(a) and 3(b) indicate that with an increase in either WO_3 layer thickness or ZnO layer thickness the peaking points of TAPs shift to lower active layer thicknesses and the number of TAPs is significantly enhanced for thin active layer ($<80 \text{ nm}$). Therefore, both WO_3 layer and ZnO layer act as an efficient optical spacer and the TAPs in thin active layer ($<80 \text{ nm}$) can be maximized when the thicknesses of WO_3 layer and ZnO layer are tailored to meet the optical resonant condition.

Finally, to obtain the optimal thickness of Alq_3 and thin Ag film, simulations have been performed to investigate the dependence of the TAPs in the active layer on the thicknesses of Alq_3 layer and Ag layer. The results of calculations are shown in Fig. 4. The maximum of TAPs occurs in the cavity devices when the thicknesses of Alq_3 layer and Ag layer thickness is equal to 50 and 13 nm. An improvement of 16.3% in TAPs is obtained when compared to the nearly

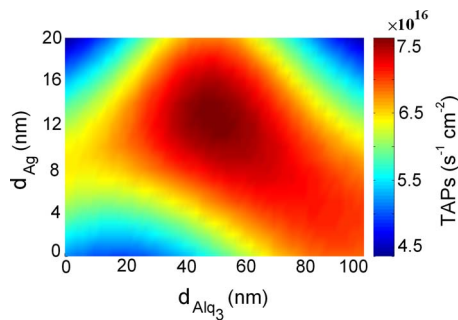


FIG. 4. (Color online) Number of TAPs in the active layer as a function of layer thicknesses of Alq_3 and transparent Ag cathode. The thicknesses of P3HT:PCBM, WO_3 , and ZnO are assumed to be 70, 10, and 10 nm, respectively.

optimized noncavity devices with a structure of Glass/ITO(105 nm)/ZnO(10 nm)/P3HT:PCBM(70 nm)/ WO_3 (10 nm)/Ag(150 nm). Moreover, there is an increase of more than 10% in the number of TAPs for cavity devices with Alq_3 layer thickness optimized to 40–60 nm and Ag layer thickness optimized to 10–16 nm.

In summary, this letter investigates the optical performance of IOSCs with metal-mirror microcavity structure. Compared to the nearly optimized IOSC devices with ITO transparent electrode, the TAPs in 70 nm-thick active layer for the cavity devices with 13 nm-thick Ag layer as transparent electrode is enhanced by 16.3% due to the cavity resonance effect. An improvement of more than 10% in TAPs is obtained when Alq_3 layer thickness is optimized to 40–60 nm and Ag layer thickness is optimized to 10–16 nm. Previous research has revealed that a silver film with thickness of 10 nm or greater has a sheet resistance equivalent or less than ITO film.¹⁴ Therefore, the thin silver transparent electrodes with thickness of 10–16 nm have both superior optical and electrical performance to ITO electrode, which

indicates that thin silver electrodes are good alternatives to ITO electrode.

- ¹C. J. Brabec, N. S. Sariciftci, and J. C. Hummelen, *Adv. Funct. Mater.* **11**, 15 (2001).
- ²H. Hoppe and N. S. Sariciftci, *J. Mater. Res.* **19**, 1924 (2004).
- ³S. E. Shaheen, D. S. Ginley, and G. E. Jabbour, *MRS Bull.* **30**, 10 (2005).
- ⁴K. M. Coakley and M. D. McGehee, *Chem. Mater.* **16**, 4533 (2004).
- ⁵C. Kim and J. S. Kim, *Opt. Express* **16**, 19987 (2008).
- ⁶M. Agrawal and P. Peumans, *Opt. Express* **16**, 5385 (2008).
- ⁷J. R. Tumbleston, D. H. Ko, E. T. Samulski, and R. Lopez, *Appl. Phys. Lett.* **94**, 043305 (2009).
- ⁸K. Tvingstedt, N. K. Persson, O. Inganäs, A. Rahachou, and I. V. Zozoulenko, *Appl. Phys. Lett.* **91**, 113514 (2007).
- ⁹A. Roy, S. H. Park, S. Cowan, M. H. Tong, S. Cho, K. Lee, and A. J. Heeger, *Appl. Phys. Lett.* **95**, 013302 (2009).
- ¹⁰J. van de Lagemaat, T. M. Barnes, G. Rumbles, S. E. Shaneen, T. J. Coutts, C. Weeks, I. Levitsky, J. Peltola, and P. Glatkowski, *Appl. Phys. Lett.* **88**, 233503 (2006).
- ¹¹K. Schulze, C. Uhrich, R. Schueppel, K. Leo, M. Pfeiffer, E. Brier, E. Reinhold, and P. Baeuerle, *Adv. Mater. (Weinheim, Ger.)* **18**, 2872 (2006).
- ¹²K. Tvingstedt and O. Inganäs, *Adv. Mater. (Weinheim, Ger.)* **19**, 2893 (2007).
- ¹³B. O'Connor, K. H. An, K. P. Pipea, Y. Zhao, and M. Shtein, *Appl. Phys. Lett.* **89**, 233502 (2006).
- ¹⁴B. O'Connor, C. Haughn, K. H. An, K. P. Pipe, and M. Shtein, *Appl. Phys. Lett.* **93**, 223304 (2008).
- ¹⁵J. Meiss, N. Allinger, M. K. Riede, and K. Leo, *Appl. Phys. Lett.* **93**, 103311 (2008).
- ¹⁶J. Meiss, M. K. Riede, and K. Leo, *Appl. Phys. Lett.* **94**, 013303 (2009).
- ¹⁷N. K. Persson, H. Arwin, and O. Inganäs, *J. Appl. Phys.* **97**, 034503 (2005).
- ¹⁸N.-K. Persson and O. Inganäs, *Sol. Energy Mater. Sol. Cells* **90**, 3491 (2006).
- ¹⁹W. Eerenstein, L. H. Slooff, S. C. Veenstra, and J. M. Kroon, *Thin Solid Films* **516**, 7188 (2008).
- ²⁰H. Hoppe, N. S. Sariciftci, and D. Meissner, *Mol. Cryst. Liq. Cryst.* **385**, 113 (2002).
- ²¹E. Palik and G. G. Dand, *Handbook of Optical Constants of Solids* (Academic, San Diego, 1998).
- ²²M. G. Hutchins, O. Abu-Alkhair, M. M. El-Nahass, and K. Abd El-Hady, *Mater. Chem. Phys.* **98**, 401 (2006).